

Mart MÄGI

Department of Mechanical Engineering  
Chalmers University of Technology  
Gothenburg, Sweden

### Introduction

In classical cylindric involute gear geometry most authors treat spur gears, helical gears and spiral (or crossed shaft-) gears as separate problems. Then it is possible to find exact solutions to some subgroups of problems, to some others only approximate solutions are known, and finally some special problems are not treated at all. If, however, a general case is studied, it seems possible to solve all problems in the field of gear geometry in general terms, either exactly in closed form or as infinite series.

The general case, mentioned above, consists of two arbitrary helical gears in mesh, having the same pitch in the normal direction, but different helix angles. That means in reality a spiral gear drive. The helical gear case is obtained if the helix angles are chosen equal but of opposite signs and for the spur gear case the helix angles are zero. The external and internal gear cases may sometimes be unified by introducing a negative number of teeth, but in general a double sign convention must be used to obtain unified formulae.

In the present paper two problems are treated in a general way: the tooth thickness of one gear wheel and the center distance of two gear wheels in conjugate action.

This leads in both cases to minimum value problems, the solution of which in general must be expressed as infinite series. When these solutions are specialized to the spur gear case, well-known solutions are obtained and the close relation between the spur, helical and spiral gear cases may be understood.

The series solutions, furthermore, give an estimation of the error involved in using - as an approximation - spur gear formulae for helical and spiral gear cases. Such approximations are discussed in terms of virtual numbers of teeth.

Here the treatment is limited to perfect gears of cylindric, involute type and the conjugate action is assumed to be backlash-free. (The case of backlash may be treated as a backlash-free case with somewhat modified tooth thicknesses.)

Differing methods are used in different countries when gears are to be specified: e.g. in most of Europe the module system is used, and in the Anglo-American countries two types of the pitch system dominate. In the present

work a third system is used, developed from the basic quantities of a gear, and the methods used here are introduced to the reader in a separate section.

Also the notation in gearing literature is different, not only from country to country, but sometimes also from author to author in the same country. These circumstances have encouraged the present author to introduce a new notation principle in the following section. The notation may look unfamiliar to most readers, but it has some advantages when dealing with gear geometry problems: all lengths are denoted by small Latin letters, all non-dimensional quantities are denoted by Greek letters and the rest by capital Latin letters. The subscript system is used to define radial levels and principal directions.

### Notation

#### Symbols

c	center distance
d	diameter
f	face width
h	tooth height
k	chordal thickness of tooth
p	pitch
r	radius
t	circular thickness of tooth
x	displacement of basic rack
$\alpha$	special ratio of teeth
$\epsilon$	contact ratio
$\theta$	half centiangle of tooth ( $= \frac{t}{d}$ )
v	number of teeth
$\tilde{t}$	rate of addendum modification (correction)
$\tilde{\epsilon}$	ratio of corrections and numbers of teeth
$\phi$	pressure angle
$\psi$	helix angle
A, B	beginning/end of contact
T	pitch point

#### Subscripts

a	axial plane
b	base cylinder
f	fillet-involute junction
n	normal plane
o	referring to standard basic rack
r	root cylinder
t	transverse plane, tip cylinder
1	referring to special gear (e.g. the pinion)
2	referring to special gear (e.g. the external or internal gear)

#### Superscripts

x	extreme value
v	virtual, alternative

## Basic Gear Data and some General Relationships

### Basic Gear Data

The most essential parts of a gear, the tooth surfaces, are uniquely defined by four quantities:

- $d_b$  = diameter of the base cylinder
- $t_{bt}$  = tooth thickness on the base cylinder in the transverse plane (direction)
- $v$  = number of teeth
- $\phi_b$  = helix angle on the base cylinder

These four quantities are here called the primary quantities in the Basic system. The contrast between the Basic system, presented here, and the various technical systems in use, e.g. the module and the pitch systems, must be pointed out. In the latter systems the tooth surfaces are defined via a basic rack, where the gear shape is the sole solution to the basic rack and its position, but inversely one specified gear may be defined via a manifold of different racks. The Basic system, however, is unique.

The extension of the tooth surfaces is limited by some secondary quantities:

- $f$  = face width
- $d_t$  = diameter of the tip cylinder
- $d_f$  = diameter of the cylinder through the fillet-involute junction

In order to enable the calculation of tip clearance

- $d_r$  = diameter of the root cylinder

may be added to the secondary gear data.

### Basic Rack

It is known from elementary literature on gears that a transverse section of an arbitrary gear co-operates with a basic rack profile as shown in Fig. 1. The basic rack is defined by the pitch  $p_t$  and the profile angle  $2\phi_t$  (both in the transverse direction). Possible points of contact lie on two lines (planes) of action for the leading and trailing contacts respectively. The rotation of the gear and the translation of the rack are connected to each other via the pitch cylinder and the pitch plane. The pitch diameter  $d$  is

$$d = \frac{d_b}{\cos \phi_t} \quad \text{.....Eq. 1}$$

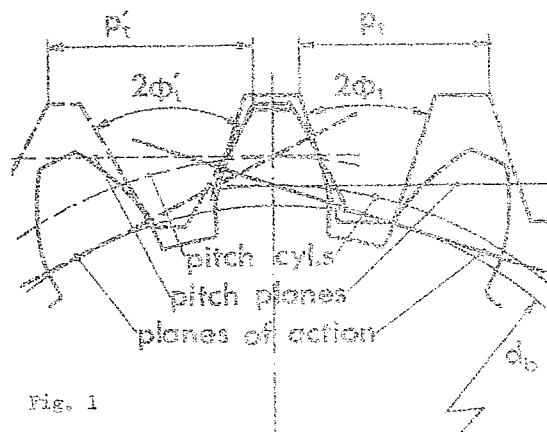


Fig. 1

Fig. 1 also shows the possibility of co-operation between the same gear, but another basic rack profile (dotted). The perpendicular

distance between the rack profile lines must, however, be unchanged and equal to the pitch on the base cylinder

$$p_t \cos \phi_t = p_t' \cos \phi_t' = p_{bt} \quad \text{.....Eq. 2}$$

The helical gear is equivalent to a twisted spur gear, and is thus able to co-operate with a basic rack which is sheared. The twisted helix angle on the pitch cylinder must be the same as the shear angle of the basic rack.

### Angular Relationships

The axial pitch  $p_a$  of a helical gear must be unchanged for all diameters, thus

$$p_a = \frac{\pi d}{v} \cot \psi = \frac{\pi d_b}{v} \cot \phi_b$$

which, with the aid of Eq. 1, gives the helix angle  $\psi$  at an arbitrary diameter  $d$

$$\tan \psi = \frac{\tan \phi_t}{\cos \phi_t} \quad \text{.....Eq. 3}$$

The pressure angle is defined as the angle between the tooth surface normal and a tangential plane through the point considered. If the angle is projected on the transverse plane, the pressure angle at the pitch point  $T$  is equal to half the profile angle of the basic rack,  $\phi_t$ .

Every basic rack which has been exposed to shear contains a normal section as seen in Fig. 2. The profile of such a normal section is principally the same as of any transverse section, but the pitch and profile angles are changed:

$$p_n = p_t \cos \psi \quad \text{.....Eq. 4}$$

$$\tan \phi_n = \cos \psi \tan \phi_t \quad \text{.....Eq. 5}$$

In the normal plane the pressure angle at the pitch point is analogously equivalent to the profile angle. The normal plane at a point is defined as a plane perpendicular to the helix through the point.

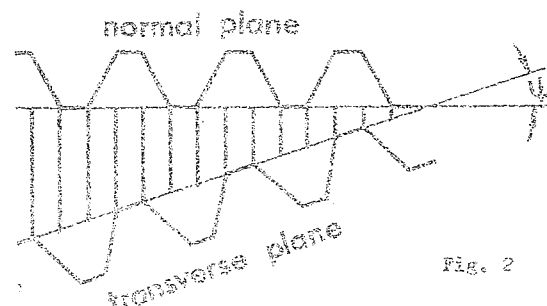


Fig. 2

### General Remarks

A basic rack is defined by its pitch and profile angle in the normal plane. A specified gear may co-operate with a manifold of basic racks, the base pitch of which must be the same, i.e.

$$p_n \cos \phi_n = p_n' \cos \phi_n' = p_{bn} \quad \text{.....Eq. 6}$$

Every basic rack, satisfying Eq. 6, co-operates with the gear at various pitch radii and thus at various helix angles and with various profile angles in the transverse plane.

Only the base helix angle is unchanged on a gear. The other angles  $\phi_t$ ,  $\phi_n$  and  $\psi$  vary with the radial level and are mutually related to each other as is evident from Eqs 1, 3 and 5. Other similar relationships may be obtained from Fig. 3.

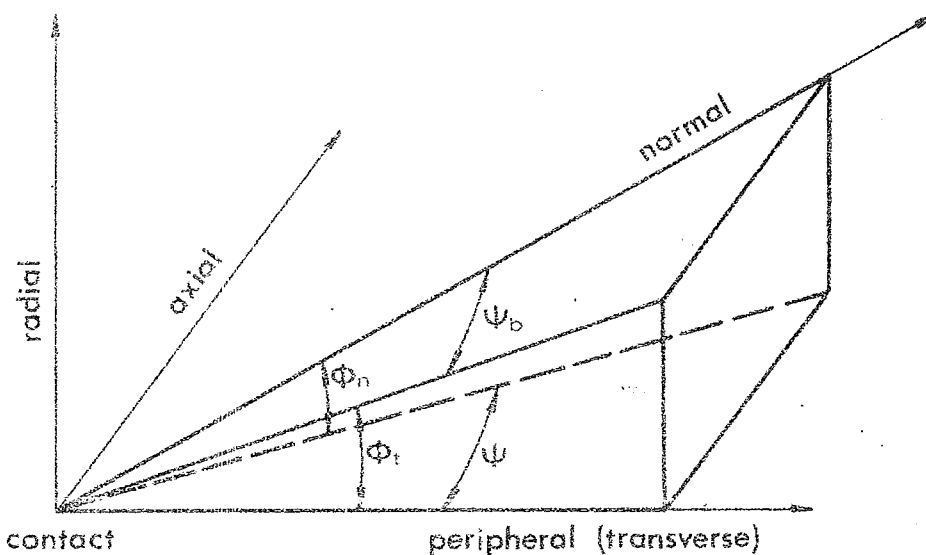


Fig. 3

### The Tooth Thickness

The tooth thickness may be considered either as an arc ( $t$ ) or as a chord ( $k$ ), where arc here may mean a distance between two points measured upon a cylindrical surface and chord may mean the shortest distance between two points on a cylinder. The circular and chordal tooth thicknesses coincide for basic racks. Additionally, the tooth thickness may be measured in the transverse or normal directions.

### The Circular Tooth Thickness

The circular tooth thickness in the transverse direction,  $t_t$ , may be determined at any diameter  $d$  of the wheel by the well-known relation

$$\left. \begin{aligned} t_t &= d \left( \frac{t_b}{d_b} \mp \text{inv} \phi_t \right) \\ \cos \phi_t &= \frac{d_b}{d} \end{aligned} \right\} \dots \dots \dots \text{Eq. 7}$$

where the upper sign is for external, the lower sign for internal gearing, and the involute function is

$$\text{inv} \phi = \tan \phi - \phi$$

The circular tooth thickness in the normal direction  $t_n$  is then

$$t_n = t_t \cos \psi \dots \dots \dots \text{Eq. 8}$$

where  $\psi$  and  $\phi_t$  are related via Eq. 3.

### The Chordal Tooth Thickness

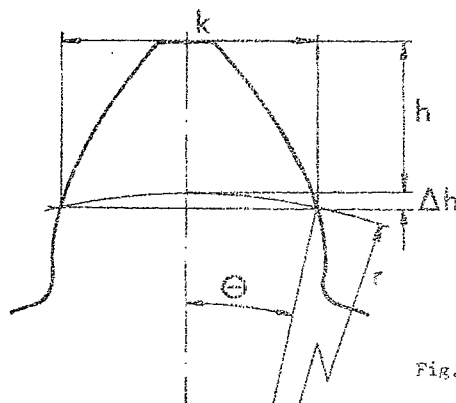


Fig. 4

The chordal tooth thickness is of interest, when the tooth thickness on the diameter  $d$  is to be measured by a calliper. For spur gears the chord  $k$  and the height increment  $\Delta h$  are easily defined as seen in Fig. 4, and calculated as

$$k = 2r \sin \theta = d \sin \frac{t}{d} \dots \dots \dots \text{Eq. 9}$$

$$\Delta h = r(1 - \cos \theta) = \frac{d}{2} (1 - \cos \frac{t}{d}) \dots \dots \dots \text{Eq. 10}$$

In the case of helical gears the chord in the transverse plane is easy to calculate, but almost impossible to measure with good accuracy. Depending upon the calliper inclination varying values of  $k$  are measured. Obviously a minimum value must exist, which may be measured with satisfactory accuracy, and this is calculated as follows.

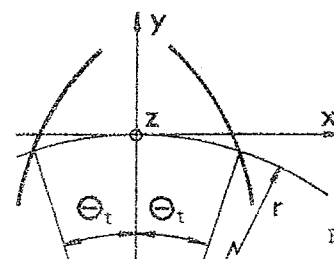


Fig. 5

The trace of a tooth surface on an arbitrary cylinder of radius  $r$ , concentric with the gear axis, being a helix with the angle  $\psi$ , is represented analytically in an xyz-coordinate system according to Fig. 5, giving for one of the tooth surfaces

$$\begin{aligned} x &= r \sin \theta \\ y &= -r(1 - \cos \theta) \\ z &= r\zeta \end{aligned}$$

where  $\theta$  and  $\zeta$  are parameters connected to each other via

$$\theta = \theta_t - \zeta \tan \psi$$

Then an arbitrary chord  $k$  between one point on each helix has the magnitude

$$k = 2\sqrt{x^2 + z^2} = 2r \sqrt{\sin^2 \theta + \zeta^2} \dots \dots \dots \text{Eq. 11}$$

The minimum chord is obtained, when the function  $f(\theta)$  is a minimum, where

$$f(\theta) = \sin^2 \theta + c^2 \sin^2 \theta + \frac{(\theta_t - \theta)^2}{\tan^2 \theta}$$

The minimum value is obtained from

$$f'(\theta) = 2 \sin \theta \cos \theta - \frac{2(\theta_t - \theta)}{\tan^2 \theta} = 0 \quad \dots \text{Eq. 12}$$

The value of  $\theta$ , satisfying Eq. 12, is denoted by  $\theta^*$ , and is an implicit function of  $\theta_t$ .

$$\theta_t = \theta^* + \sin^2 \theta^* \cos^2 \theta^* \tan^2 \theta^* \quad \dots \text{Eq. 13}$$

In most cases  $\theta^*$  is a small angle. Maclaurin's expansion and series reversion of Eq. 13 give

$$\theta^* = \theta_t \cos^2 \theta_t + \frac{2}{3} \theta_t^3 \sin^2 \theta_t \cos^6 \theta_t - \frac{2}{15} \theta_t^5 + \dots \quad \dots \text{Eq. 14}$$

Substitution of the power series solution, Eq. 14, into Eq. 11 gives

$$\frac{k^*}{2\theta_t \cos \theta_t} = \frac{k}{t} = 1 - \frac{(\theta_t \cos^3 \theta_t)^2}{3!} + \frac{1-24 \tan^2 \theta_t}{5!} (\theta_t \cos^3 \theta_t)^4 + \dots \quad \dots \text{Eq. 15}$$

In a similar way the height increment  $\Delta h$  is calculated. With the previous notation it is

$$\Delta h = r \psi (1 - \cos \theta)$$

and when the solution of  $\theta^*$  in Eq. 14 is substituted, then

$$\frac{\Delta h^*}{2r \theta_t \cos \theta_t} = \frac{\Delta h}{t} = \frac{\theta_t \cos^3 \theta_t}{2!} - \frac{1-16 \sin^2 \theta_t}{4!} (\theta_t \cos^3 \theta_t)^3 + \dots \quad \dots \text{Eq. 16}$$

#### Conjugate Action of Two Arbitrary Gear Wheels

Two gear wheels require for conjugate action the same pitch in the normal direction on their base cylinders, i.e.,

$$p_{bn1} = p_{bn2}$$

Here the subscripts 1 and 2 are chosen independent of the gear size and power flow direction. The following discussions are formally valid for both external and internal wheel, if any, and the upper sign implies external - the lower sign internal - gearing. In the internal case, however, only the parallel shaft case,  $\psi_{b1} = -\psi_{b2}$ , is possible.

Both the wheels with known basic gear data may co-operate with an imaginary basic rack as described in a former section. The imaginary rack is defined as a profile without thickness, capable of co-operating with a gear with both of its sides. The rack must satisfy the following condition:

$$p_{bn} = p_n \cos \psi_n = p_{bn1} = p_{bn2} \quad \dots \text{Eq. 17}$$

At first one of the gears is put in backlash-free contact with the imaginary rack. The shaft position is then known relative to the rack, regarding the center distances and shaft angle.

All possible points of contact between the

rack and the wheel lie in two planes of action and the parts are kinematically coupled through the pitch plane and the pitch cylinder, the position of which are known from former sections.

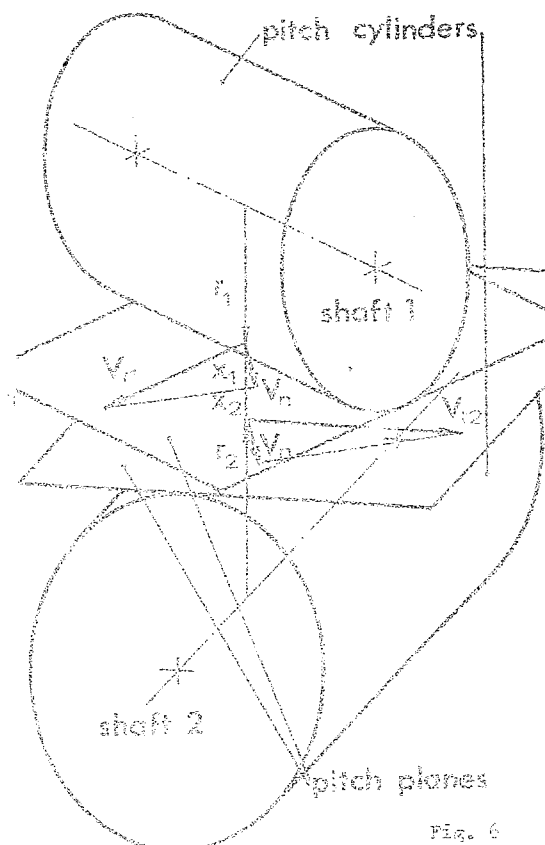
The described procedure is then repeated with the other wheel. In the case of external gears the wheels co-operate with the imaginary rack from opposite sides, and in the internal case from the same side.

The two wheels must touch each other in such points, where they are in simultaneous contact with the imaginary rack. Such points must lie in the planes of action for both the wheels, thus these points must lie on the line of intersection between the planes. One of these lines of action is obtained for the leading point of contact, another for the trailing point. Thus the gear wheels operate without backlash.

In general, when the axes of the gears are not parallel, i.e.,  $\psi_{b1} \neq \psi_{b2}$ , the planes of action are not parallel either, and an intersection line always occurs. If, however, the shafts are parallel, the planes of action either coincide or never intersect. In the first case, the gears work with line contact, in the other case the gear teeth are separated by backlash.

The kinematic coupling is shown in Fig. 6, where it is seen that in general the pitch planes for both the wheels do not coincide, but are separated by a distance  $x_2 - x_1$ . The velocity  $V$  of the pitch planes in the normal direction must be equal for both the wheels, and be a component of the total velocity in the transverse direction.

The line of action for the leading point of contact, denoted by AB, and the trailing point, denoted by A'B' (dotted) is shown in Fig. 7, where four views are seen: both the transverse planes, the normal plane and the pitch plane. The full-scale length of AB is found in the normal plane view.



In order to maintain the mutual contact for every position of the wheels,  $\overline{AB} > p_{bn}$  or in terms of the contact ratio  $\epsilon$

$$\epsilon = \frac{\overline{AB}}{p_{bn}} > 1 \quad \dots\dots\dots \text{Eq. 18}$$

The whole line of action is used, only if  $\overline{AB}$  is contained within the face widths of the wheels:

$$r > \overline{AB} \sin \psi_b$$

If backlash-free action is desired, both  $\overline{AB}$  and  $\overline{A'B'}$  must be contained within the somewhat larger face widths  $r'$ .

It must be pointed out that the solution shown in Fig. 7 is only one of many possible. If a somewhat changed imaginary rack were taken as a basis for the consideration the whole solution would be somewhat changed but principally the same.

A similar discussion, but only for one of the lines of action and only one shape of the rack, has previously been presented by BUCKINGHAM, ref. 1.

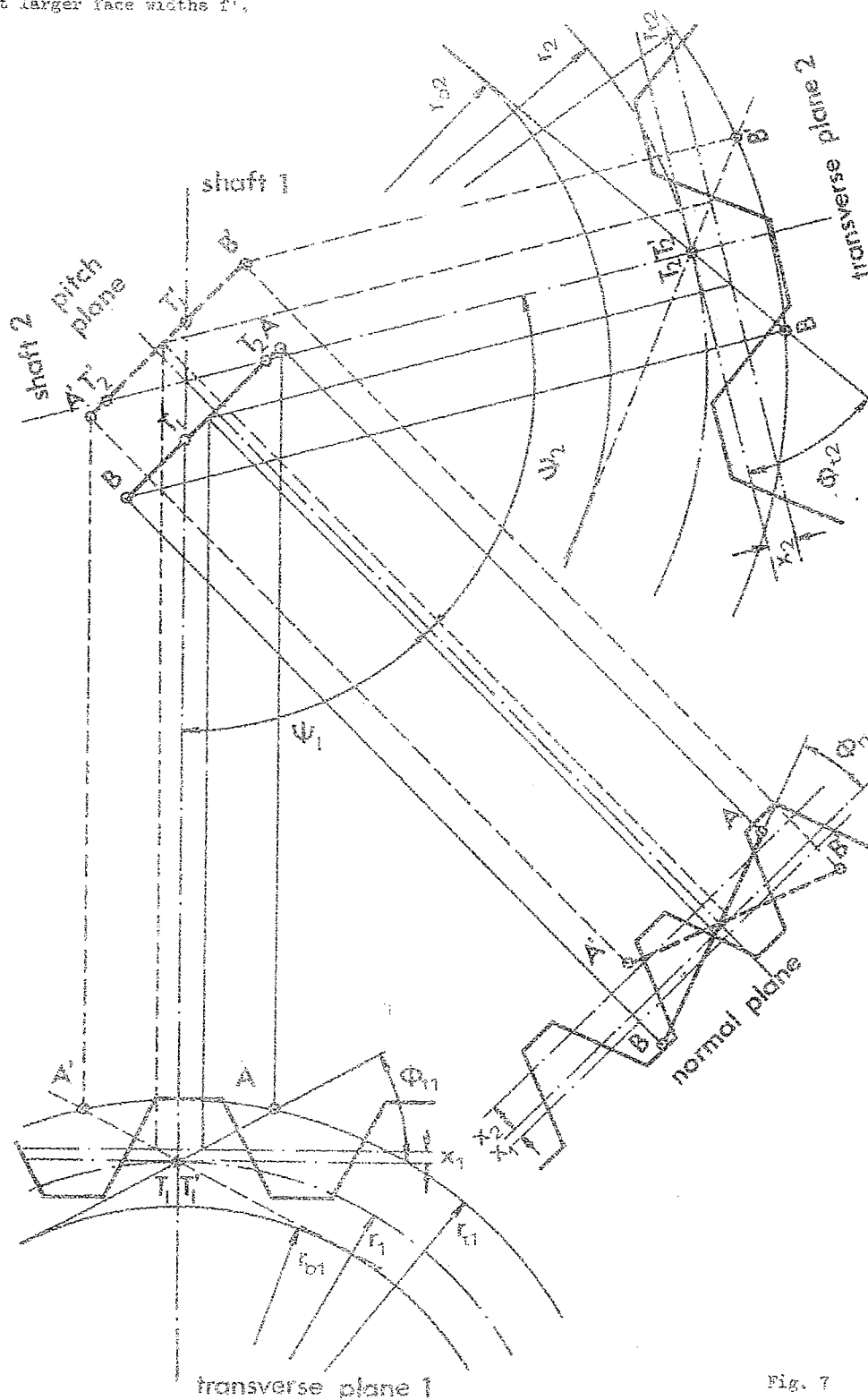


Fig. 7

# Minimum Center Distance (M.C.D.)

## General Expression for Center Distance

A general expression for the center distance  $c$  is obtained by adding the pitch radii and the displacements of the pitch cylinders from the mid-line of the imaginary rack. For a pair of wheels making backlash-free contact,  $c$  is then

$$c = r_2 + r_1 + x_2 + x_1 \quad \text{.....Eq.19}$$

The basic gear data for the wheels is considered as given. Then it is possible to express Eq. 19 in terms of the basic gear data and the quantities  $\phi_n$  and  $p_n$  of any basic rack that satisfies Eq. 17.

With the aid of Fig. 3, the pitch helix angles  $\psi$  are obtained from

$$\cos \phi_n = \frac{\sin \psi_{b1}}{\sin \psi_1} = \frac{\sin \psi_{b2}}{\sin \psi_2} \quad \text{.....Eq.20}$$

The pitch radii are obtained from

$$r = \frac{d_b}{2 \cos \phi_n} \quad \text{.....Eq.21}$$

The distance between the pitch cylinders,  $x_2 + x_1$ , is determined by comparing the sum of the thicknesses of the teeth on the pitch cylinders with the pitch of the imaginary rack. The thickness in the normal direction,  $t_n$ , is obtained from Eq. 8, or rewritten

$$t_n = t_t \cos \psi = (t_{bt} + d_b \text{inv} \phi_t) \frac{\cos \psi}{\cos \phi_t} \quad \text{...Eq.22}$$

Fig. 3 gives, however

$$\frac{\cos \psi}{\cos \phi_t} = \frac{\cos \psi_b}{\cos \phi_n} \quad \text{.....Eq.23}$$

thus giving

$$t_n = (t_{bt} + d_b \text{inv} \phi_t) \frac{\cos \psi_b}{\cos \phi_n} \quad \text{.....Eq.24}$$

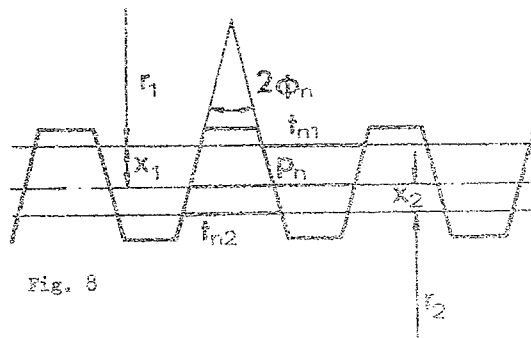


Fig. 8

As seen from Fig. 8 (an external case) the distance  $x_2 + x_1$  is

$$x_2 + x_1 = \frac{t_{n1} + t_{n2} - p_n}{2 \tan \phi_n} \quad \text{.....Eq.25}$$

The normal pitch of the imaginary rack must suit both wheels, thus

$$\begin{aligned} \frac{p_n}{\cos \phi_n} &= \frac{\pi d_b \cos \psi_b}{v \cos \phi_n} \\ &= \frac{\pi d_{b1} \cos \psi_{b1}}{2 v_1 \cos \phi_n} + \frac{\pi d_{b2} \cos \psi_{b2}}{2 v_2 \cos \phi_n} \quad \text{.....Eq.26} \end{aligned}$$

Substituting Eqs 23, 25 and 24, 26 in Eq. 19 gives

$$\begin{aligned} c &= \frac{d_{b2}}{2 \cos \phi_{t2}} + \frac{d_{b1}}{2 \cos \phi_{t1}} + \frac{1}{2 \sin \phi_n} \\ &\cdot \left( (t_{bt2} - d_{b2} (\frac{\pi}{2 v_2} + \text{inv} \phi_{t2})) \cos \psi_{b2} + \right. \\ &\left. + (t_{bt1} - d_{b1} (\frac{\pi}{2 v_1} + \text{inv} \phi_{t1})) \cos \psi_{b1} \right) \quad \text{Eq.27} \end{aligned}$$

where the angular relationships are connected via Eq. 20.

## Minimum Center Distance

The center distance is according to Eq. 27 dependent on the rack shape which is chosen. It is a function of the angle  $\phi_n$ . Obviously there must exist an extreme value for the center distance, which must be a minimum in the external case. This value is obtained by differentiating the center distance with respect to the rack pressure angle.

Remembering from Fig. 3 that

$$\sin \phi_t = \frac{\sin \phi_n}{\cos \psi_b} \quad \text{.....Eq.28}$$

giving

$$\frac{d \phi_t}{d \phi_n} = \frac{\cos \phi_n}{\cos \phi_t \cos \psi_b}$$

and

$$\frac{d}{d \phi} (\text{inv} \phi) = \frac{d}{d \phi} (\tan \phi - \phi) = \tan^2 \phi$$

the following is obtained:

$$\begin{aligned} \frac{dc}{d \phi_n} &= \frac{d_{b2} \sin \phi_{t2} \cos \phi_n}{2 \cos^3 \phi_{t2} \cos \psi_{b2}} + \frac{d_{b1} \sin \phi_{t1} \cos \phi_n}{2 \cos^3 \phi_{t1} \cos \psi_{b1}} \\ &- \frac{d_{b2} \sin^2 \phi_{t2} \cos \phi_n}{2 \sin \phi_n \cos^3 \phi_{t2}} + \frac{d_{b1} \sin^2 \phi_{t1} \cos \phi_n}{2 \sin \phi_n \cos^3 \phi_{t1}} \\ &+ \frac{\cos \phi_n}{2 \sin \phi_n} \left( (d_{b2} (\frac{\pi}{2 v_2} + \text{inv} \phi_{t2}) - t_{bt2}) \cos \psi_{b2} + \right. \\ &\left. + (d_{b1} (\frac{\pi}{2 v_1} + \text{inv} \phi_{t1}) - t_{bt1}) \cos \psi_{b1} \right) \quad \text{Eq.29} \end{aligned}$$

Eq. 26 cancels the first four terms in Eq. 29, and by using Eq. 26 the derivative is simplified to

$$\begin{aligned} \frac{dc}{d \phi_n} &= \frac{d_{b1} \cos \psi_{b1} \cos \phi_n}{2 v_1 \sin \phi_n} \left( v_2 (\frac{\cos \phi_n}{d_{b2}} + \text{inv} \phi_{t2}) + \right. \\ &\left. + v_1 (\frac{t_{bt1}}{d_{b1}} - \text{inv} \phi_{t1}) - \pi \right) \quad \text{.....Eq.30} \end{aligned}$$

The extreme value is obtained when

$$\frac{dc}{d \phi_n} = 0$$

giving the M.C.D. condition

$$\left. \begin{aligned} v_2 \left( \frac{t_{b2}}{d_{b2}} \sin \psi_{o2}^N + v_1 \left( \frac{t_{b1}}{d_{b1}} \sin \psi_{o1}^N \right) \right) &= \\ \frac{\sin \psi_{o1}^N}{\sin \psi_{o2}^N} &= \frac{\cos \psi_{o2}}{\cos \psi_{o1}} \end{aligned} \right\} \quad \text{.....Eq. 31}$$

The M.C.D. solution corresponds geometrically to the case, when the two pitch planes (see Fig. 6) coincide. The minimum center distance is then

$$c^N = \frac{d_{o2}}{\cos \psi_{o2}^N} + \frac{d_{o1}}{\cos \psi_{o1}^N} \quad \text{.....Eq. 32}$$

For the special case, when  $\psi_{o1}^N = -\psi_{o2}^N$ , i.e. parallel shafts, the solution in earlier literature is known as the FURBER equation. In that case it is possible to solve the common pressure angle  $\psi^N$  in a closed form

$$\sin \psi_{ot}^N = \frac{v_2 \frac{t_{b2}}{d_{b2}} + v_1 \frac{t_{b1}}{d_{b1}}}{v_2 + v_1} \quad \text{.....Eq. 33}$$

or in terms of standard rack dimensions and correction factors  $\xi$ :

$$\sin \psi_{ot}^N = \sin \psi_{ot} + \frac{\xi_{o2} + \xi_{o1}}{v_2 + v_1} 2 \tan \psi_{on} \quad \text{...Eq. 34}$$

where

$$\xi = \frac{m}{d_n}$$

Methods for Numerical Solution of the M.C.D. equation

Besides the trial and error method, when solving the general M.C.D. condition 31, a series expansion method leads to an explicit solution.

A start is made from the data obtained when the gears are in conjugate action with a standard (or known) imaginary rack. These are denoted by the subscript o.

At the M.C.D. position the angles are somewhat changed from the standard angles according to

$$\left. \begin{aligned} \psi_o &= \psi_{ot} + \Delta \psi_o \\ \psi_n &= \psi_{on} + \Delta \psi_n \end{aligned} \right\} \quad \text{.....Eq. 35}$$

The relation between  $\Delta \psi_o$  and  $\Delta \psi_n$  is obtained from a modified form of Eq. 26

$$\sin(\psi_{ot} + \Delta \psi_o) = \frac{\sin(\psi_{on} + \Delta \psi_n)}{\cos \psi_o} \quad \text{....Eq. 36}$$

which after Taylor's expansions and series reversion gives

$$\begin{aligned} \Delta \psi_n &= 1 - \left( \frac{1}{\sin^2 \psi_{on}} + \frac{3}{2} (a_1 \tan^2 \psi_{o1} + a_2 \tan^2 \psi_{o2}) \right) \tan^2 \psi_{on} L^2 + \left( \frac{5-2 \sin^2 \psi_{on}}{3 \sin^4 \psi_{on}} - \frac{7-2 \sin^2 \psi_{on}}{2 \sin^2 \psi_{on}} (a_1 \tan^2 \psi_{o1} + a_2 \tan^2 \psi_{o2}) \right) \\ &+ \frac{3}{8} (a_1 \tan^2 \psi_{o1} + a_2 \tan^2 \psi_{o2})^2 - \frac{5}{2} (a_1 \tan^4 \psi_{o1} + a_2 \tan^4 \psi_{o2}) \tan^2 \psi_{on} L^3 + \dots \end{aligned} \quad \text{.....Eq. 41}$$

$$\begin{aligned} \Delta \psi_o &= \frac{1}{\cos \psi_o} \Delta \psi_n + \frac{\tan \psi_{on} \tan^2 \psi_o}{2 \cos \psi_o} (\Delta \psi_n)^2 + \\ &+ \frac{3 \tan^2 \psi_{on} \tan^2 \psi_o + \sin^2 \psi_o}{6 \cos^3 \psi_o} (\Delta \psi_n)^3 + \dots \end{aligned} \quad \text{Eq. 37}$$

Eq. 31 may be rewritten in terms of standard rack quantities and correction factors

$$\begin{aligned} v_1 (\sin \psi_{o1} - \sin \psi_{ot1}) + v_2 (\sin \psi_{o2} - \sin \psi_{ot2}) &= \\ = 2(\xi_{o1} - \xi_{o2}) \tan \psi_{on} \end{aligned} \quad \text{.....Eq. 38}$$

The difference  $(\sin \psi_{ot} - \sin \psi_o)$  is calculated after Taylor's expansion of  $\sin(\psi_o + \Delta)$  and series reversion, giving

$$\begin{aligned} \sin \psi_o - \sin \psi_{ot} &= \tan^2 \psi_{ot} \Delta \psi_o + \frac{\tan \psi_{ot}}{2 \cos^3 \psi_{ot}} (\Delta \psi_o)^2 + \\ &+ \frac{1+2 \sin^2 \psi_{ot}}{3 \cos^5 \psi_{ot}} (\Delta \psi_o)^3 + \dots \end{aligned} \quad \text{.....Eq. 39}$$

Substituting Eqs 37 and 39 into Eq. 38, the rate of correction  $(\xi_{o1} - \xi_{o2})$  is expressed as a power series of  $\Delta \psi_o$ . After series reversion and following substitutions

$$\left. \begin{aligned} L &= \frac{\xi_{o2} - \xi_{o1}}{v_2 + v_1} = \frac{2}{\tan \psi_{on}} \\ a_1 &= \frac{\frac{v_2}{\cos^3 \psi_{o2}} + \frac{v_1}{\cos^3 \psi_{o1}}}{\frac{v_2}{\cos^3 \psi_{o2}} + \frac{v_1}{\cos^3 \psi_{o1}}} \\ a_2 &= \frac{\frac{v_2}{\cos^3 \psi_{o2}} + \frac{v_1}{\cos^3 \psi_{o1}}}{\frac{v_2}{\cos^3 \psi_{o2}} + \frac{v_1}{\cos^3 \psi_{o1}}} \end{aligned} \right\} \quad \text{Eq. 40}$$

the change of the pressure angle,  $\Delta \psi_o$  (in radians), is obtained in an explicit form as a power series of  $L$

The center distance, when two wheels are in conjugate action with an imaginary standard rack, would be denoted by  $c_0$  and calculated from the following equation (compare Eq. 19)

$$c_0 = r_{o2} + r_{o1} + x_{o2} - x_{o1} \quad \dots\dots\dots \text{Eq. 42}$$

The influence,  $\Delta c$ , on the center distance, when the pressure angle of the imaginary rack is changed, is in the first approximation obtained from Eq. 30, which, remembering the meaning of the large brackets, is

$$\Delta c = \frac{x_{o1} + x_{o2}}{\tan \phi_{on}} \Delta \phi_n \quad \dots\dots\dots \text{Eq. 43}$$

In order to obtain the M.C.D.-value,  $\Delta \phi_n$  from Eq. 41 is to be substituted, giving in the first approximation

$$\Delta c = \frac{x_{o1} + x_{o2}}{\tan \phi_{on}} \frac{-2(\xi_{o2} + \xi_{o1})^2 p_{on}}{\pi(v_2' + v_1') \tan^2 \phi_{on}} \quad \dots\dots\dots \text{Eq. 44}$$

From Eq. 44 it is seen that  $\Delta c$  is always negative, proving that the extreme value of the center distance according to Eq. 32 must be a minimum value.

The influence of pressure angle change on the shaft angle - in terms of the pitch helix angles - is investigated in a similar way.

A small change  $\Delta \psi$  in the helix angle is assumed, corresponding to a small change  $\Delta \phi$  in the normal pressure angle. Starting from a modified form of Eq. 20

$$\cos(\phi_{on} + \Delta \phi_n) = \frac{\sin \phi_n}{\sin(\psi_o + \Delta \psi)} \quad \dots\dots \text{Eq. 45}$$

Taylor's expansions and series reversion give

$$\begin{aligned} \frac{\Delta \phi}{\tan \phi_o} = & \tan \phi_{on} \Delta \phi_n + \frac{1 - \frac{\sin^2 \phi_{on}}{\cos^2 \psi_o}}{2 \cos^2 \phi_{on}} (\Delta \phi_n)^2 + \\ & + \left( (1 + 3 \tan^2 \psi_o) \left( 1 + \frac{\sin^2 \phi_{on}}{2 \cos^2 \psi_o} \right) + 4 \right) \cdot \\ & \cdot \frac{\sin^2 \phi_{on}}{6 \cos^3 \psi_o} (\Delta \phi_n)^3 \dots\dots \end{aligned} \quad \dots\dots \text{Eq. 46}$$

The shaft angle change for the M.C.D. case is obtained by substituting the solution from Eq. 41 into Eq. 46, giving a first approximation

$$\begin{aligned} \Delta \phi_1 + \Delta \phi_2 = & \tan \phi_{on} (\tan \psi_{o1} + \tan \psi_{o2}) \Delta \phi_n = \\ = & \frac{2(\xi_{o2} + \xi_{o1})}{v_2' + v_1'} (\tan \psi_{o1} + \tan \psi_{o2}) \quad \dots\dots \text{Eq. 47} \end{aligned}$$

Summing up the results, it is found that the shaft angle may be moved from the M.C.D. position in either direction. In both cases the shaft center distance is increased.

#### Virtual Number of Teeth

The series solutions of the two minimum problems as appearing in Eq. 15 and Eq. 16 for the chordal tooth thickness and in Eq. 41 for the angle  $\phi_n^*$  at minimum center distance may be specialized to the spur gear case by putting  $\psi = 0$ , which gives

$$\frac{k^*}{t} = 1 - \frac{\theta^2}{3!} + \frac{\theta^4}{5!} \quad \dots\dots\dots \text{Eq. 48}$$

$$\frac{\Delta h}{t} = \frac{\theta}{2!} - \frac{\theta^3}{4!} + \dots\dots \quad \dots\dots\dots \text{Eq. 49}$$

$$\begin{aligned} \phi_n^* = & \phi_o + \frac{\xi_{o2} + \xi_{o1}}{v_2' + v_1'} \frac{2}{\tan \phi_o} + \frac{(\xi_{o2} + \xi_{o1})^2}{(v_2' + v_1')^2} \frac{4 \cos \phi_o}{\sin^3 \phi_o} + \\ & + \frac{(\xi_{o2} + \xi_{o1})^3}{(v_2' + v_1')^3} \frac{8 \cos \phi_o (5 - 2 \sin^2 \phi_o)}{3 \sin^5 \phi_o} + \dots\dots \end{aligned} \quad \dots\dots \text{Eq. 50}$$

Exact solutions in closed form are, however, known for all three of these equations as found in Eqs 9, 10 and 33.

If a virtual number of teeth  $v'$  is used in Eqs 15, 16 and 41, where

$$v' = \frac{v}{\cos^3 \psi} \quad (= \frac{v}{\cos^3 \psi}) \quad \dots\dots\dots \text{Eq. 51}$$

implying  $\theta = \theta_o \cos^3 \psi$ , the approximate and exact equations are congruent up to the first order small quantities in the series solutions. Thus, if the virtual number of teeth is used, helical gears may be treated as spur gears, and the errors that are introduced by such an approximation, are

$$\Delta k = - \frac{\cos^{10} \psi \sin^2 \psi \theta_o^4}{5} t_n \quad \dots\dots \text{Eq. 52}$$

$$\Delta(\Delta h) = \frac{2 \sin^2 \psi \theta_o^3}{3} t_n \quad \dots\dots \text{Eq. 53}$$

$$\Delta \phi_n^* = - \frac{3 \tan \phi_{on}}{2} (\alpha_1 \tan^2 \psi_{o1} + \alpha_2 \tan^2 \psi_{o2}) \theta_o^2 \quad \dots\dots\dots \text{Eq. 54}$$

The choice of the virtual number of teeth as given in Eq. 51, is in contradiction to that recommended by NIEMANN, ref. 3, where

$$v' = \frac{v}{\cos \psi_o \cos^2 \psi_o} \quad \dots\dots\dots \text{Eq. 55}$$

The approximation according to Eq. 55 is excellent for another group of problems, and for some other problems still other approximations are the most suitable. An approach for the choice of the best virtual number of teeth for various groups of problems is given by the present author in ref. 2.



## A Numerical Example

The conjugate action of two helical gears and the use of the virtual number of teeth, as described in previous sections, is elucidated in a numerical example.

ZEISE, ref. 4, has illustrated the need of non-standard spiral gear drives. For a case where  $c=50$  mm,  $\psi_1+\psi_2=90^\circ$ , gear ratio  $v_1/v_2=0.6$ , module  $m_{on}=2.5$  mm and available diametral space  $d_1 \leq 47$  mm,  $d_2 \leq 75$  mm, was suggested, by the use of virtual number of teeth, gears with data, listed in Tab. 1.

wheel	1	2
$v$	9	15
$d_b$ mm	37.489	52.669
$t_{bt}$ mm	7.263	7.618
$\psi_b$ °	47.408	36.595
$d_t$ mm	46.65	65.27

Tab. 1

For these wheels the center distance  $c$ , Eq. 27, shaft angle  $\psi_1+\psi_2$ , Eq. 20, and contact ratio, Eq. 56, are calculated for various shapes ( $\phi_n$ ) of the imaginary basic rack. The results are shown in Fig. 9. The range within which the center distance and shaft angle may vary, is limited by the condition  $c_{n1}$ .

$$c_n = \frac{AB}{P_{bn}}, \text{ where}$$

$$AB = \frac{\sqrt{r_{t1}^2 - r_{b1}^2} - r_{b1} \tan \phi_{t1}}{\cos \psi_{b1}} +$$

$$+ \frac{\sqrt{r_{t2}^2 - r_{b2}^2} - r_{b2} \tan \phi_{t2}}{\cos \psi_{b2}} - \frac{t_{n1} + t_{n2} - p_n}{2 \sin^2 \phi_n \cos \phi_n}$$

.....Eq. 56

The whole line of action for the leading point of contact is fully used, only if the face widths exceed the minimum values  $f_1, f_2$ . To avoid backlash, somewhat thicker wheels are required,  $f > f_1, f_2$ . These critical face widths are shown in Fig. 10.

The location of the lines of action, as well as the unsymmetric location of the wheels in the case of minimum face widths  $f_1, f_2$  (solid lines) is shown in Fig. 11. a/...e/ indicate some special positions and the corresponding values of  $\phi_n$  may be found from Figs 9 and 10.

The minimum center distance with corresponding shaft angle and contact ratio are also calculated by using both exact and approximate methods. The results are shown in Tab. 2 and are also plotted in Fig. 9 with small circles. In Fig. 9 is plotted, additionally, with a dotted line the case, when

$c=1$  for a virtual spur gear drive. In Tab. 2 exact solution means a trial and error solution of Eq. 31, the power series method means the use of Eq. 41, the virtual method means the use of Eq. 33 with virtual numbers of teeth, and finally corrected basic solutions mean the use of Eqs 44, 47 and 54.

## Conclusions

Methods are developed for studying the conjugate action of two arbitrary cylindric, helical, involute wheels, concerning the center distance, shaft angle, location of the lines of action and similar. A condition is derived for the minimum center distance (M.C.D.), which seems to be the natural position of two wheels in conjugate action and corresponds to the backlash-free operating position of two wheels on parallel shafts. Explicit numerical solutions for M.C.D. conditions are given as infinite power series.

The minimum chordal tooth thickness of helical gears, which is important when such teeth are measured by calliper setting, is calculated and expressed as an infinite power series.

It is shown that approximate methods, especially spur gear formulae used in combination with virtual numbers of teeth, supply a satisfactory accuracy - probably much better than the accuracy of gear measuring and cutting - when the minimum chordal tooth thickness and minimum center distance are to be calculated.

## Acknowledgements

The main part of the present paper is included in a study of gear geometry, carried out at the Institute of Machine Elements, Chalmers University of Technology, Gothenburg, Sweden, and reported in ref. 2. The present author would like to thank the head of the Institute, Professor B. Jakobsson, for his valuable positive criticism of the work.

The study has been sponsored by the Swedish Council for Applied Research.

## References

1. BUCKINGHAM, E: Analytical Mechanics of Gears; McGraw-Hill, New York 1949.
2. MAGI, M: On Geometrical Problems of Cylindric Involute Gears with Special Reference to Conjugate Action; Acta Polytechnica Scandinavica, Stockholm, to be published.
3. NIEMANN, G: Maschinenelemente, Vol. 2; Springer, Berlin 1960.
4. ZEISE, G: Korrektur von Schraubenradgetriebe; Werkstatt und Betrieb, 89(1956), Nr. 6.

	exact solution	3 term power series method	virtual method	corrected basic solution
$\phi_n$	18°42'16"	18°42'33"	18°43'18"	18°42'20"
$c$	50.012	50.014	50.022	49.995
$\psi_1+\psi_2$	90°00'51"	90°01'04"	90°01'34"	89°59'01"
$c_n$	1.731		1.736	

Tab. 2

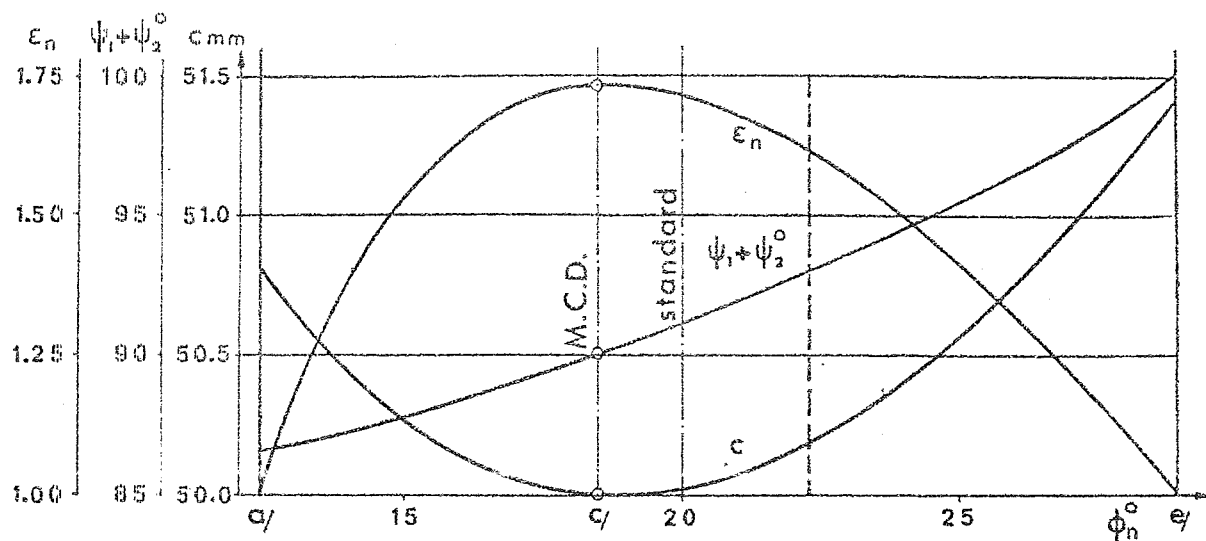


Fig. 9

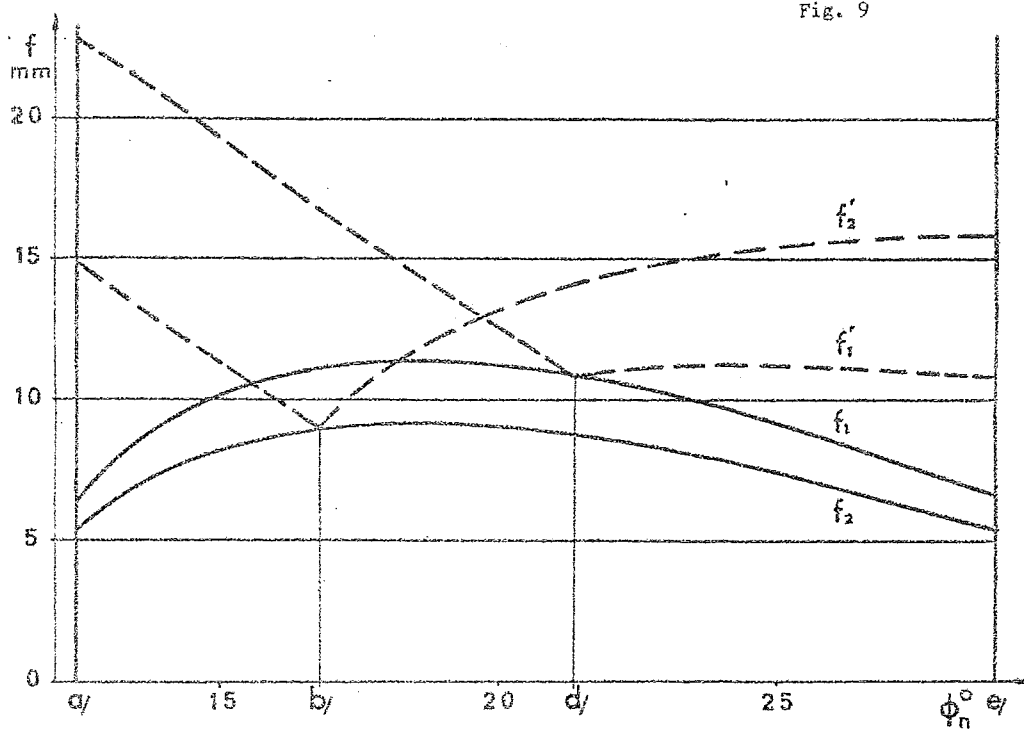


Fig. 10

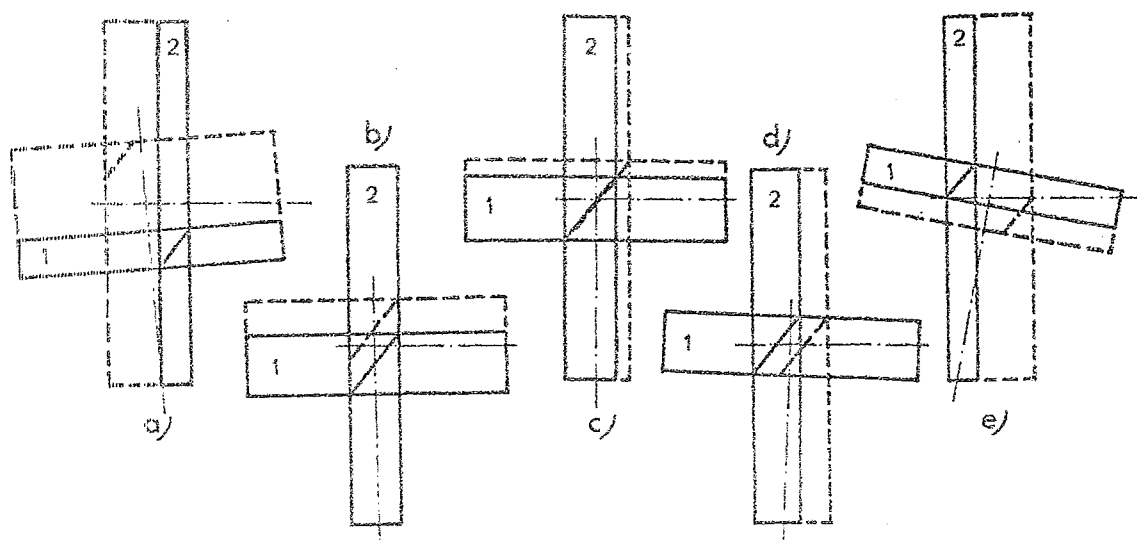


Fig. 11